SIMCor

In-Silico testing and validation of Cardiovascular IMplantable devices

Call: H2020-SC1-DTH-2018-2020 (*Digital transformation in Health and Care*)

Topic: SC1-DTH-06-2020 (*Accelerating the uptake of computer simulations for testing medicines and medical devices*)

Grant agreement No: 101017578

Deliverable 7.4

Sensitivity and uncertainty quantification toolbox

Due date of delivery: 31 March 2022

Actual submission date: 28 March 2022

Start of the project: 1 January 2021
End date: 31 December 2023

This project has received funding from the European Union's Horizon 2020 research and innovation programmeunder grant agreement N° 101017578

Reference

Name	SIMCor_D7.4_ Sensitivity and uncertainty quantification toolbox _TUE_28-03-2022
Lead beneficiary	Technische Universiteit Eindhoven (TUE)
Author(s)	Wouter Huberts (TUE)
Dissemination level	Public
Type	Report
Official delivery date	31 March 2022
Date of validation by the WP Leader	28 Mach 2022
Date of validation by the Coordinator	**28 March 2022**
Signature of the Coordinator	Jan Bruening Digital unterschrieben von Jan Bruening Datum: 2022.03.28 23:38:04 +02'00'

Version log

Issue date	Version	Involved	Comments
14/03/2022	1.0	Wouter Huberts (TUE)	First draft by TUE
20/03/2022	2.0	Jan Brüning (CHA); Lucian Itu (UTBV)	Internal review by CHA and UCL
21/03/2022	3.0	Wouter Huberts (TUE)	New version, taking into accounts comments and suggestions
25/03/2022	4.0	Anna Rizzo (LYN)	Final review and formal checking by LYN
28/03/2022	Final	Jan Brüning (CHA)	Submission by PC

Executive summary

The contents of this deliverable are presented to demonstrate the proof-of-principle of the application of uncertainty quantification and sensitivity analysis to both aortic valve stenosis and heart failure patients. Sensitivity analysis will be used extensively in SIMCor for two specific objectives: 1) assessment/ranking of relevant model parameters for the output(s) of interest, and 2) design of the selection criteria for filtering during virtual cohort creation.

This deliverable starts with the formal definition of uncertainty and sensitivity analysis that we adopted from literature. Thereafter, we will briefly explain the envisioned sensitivity analysis strategies and we will show preliminary results when applying these techniques to models with different levels of complexity and computational demands. These preliminary results demonstrate the feasibility of applying our sensitivity tools to relevant use cases. As uncertainty and sensitivity analysis are strongly related concepts, the uncertainty in model predictions follows almost directly from the sensitivity analyses applied.

Table of contents

List of figures

List of tables

Acronyms

Acronym	Full name
TAVI	Transcatheter Aortic Valve Implantation
PAPS	Pulmonary Artery Pressure Sensor
HF	Heart failure
CFD	Computational Fluid Dynamics
0D	Lumped parameter model
PWPM/1D	Pulse wave propagation model
FSI	Fluid Structure Interaction
SSI	Structure Structure Interaction
RSA	Regionalized Sensitivity Analysis
SSM	Statistical Shape Model
SGI	Sparse Grid Interpolation
UQ	Uncertainty analysis
SA	Sensitivity analysis

Definitions

In this section we first introduce the definitions of uncertainty and sensitivity analysis that we are using in SIMCor. These definitions are adopted from the definitions given by Saltelli et al.[1,2] (see also Figure 1).

Uncertainty analysis: Quantification of the uncertainty in the output(s) of interest due to uncertainties in model assumptions, parameters, and/or initial and boundary conditions, collectively referred to as model input factors.

Sensitivity analysis: In this type of analysis each fraction of the total uncertainty in model outputs will be attributed to uncertainties of the input factors and/or the interactions between uncertain input factors.

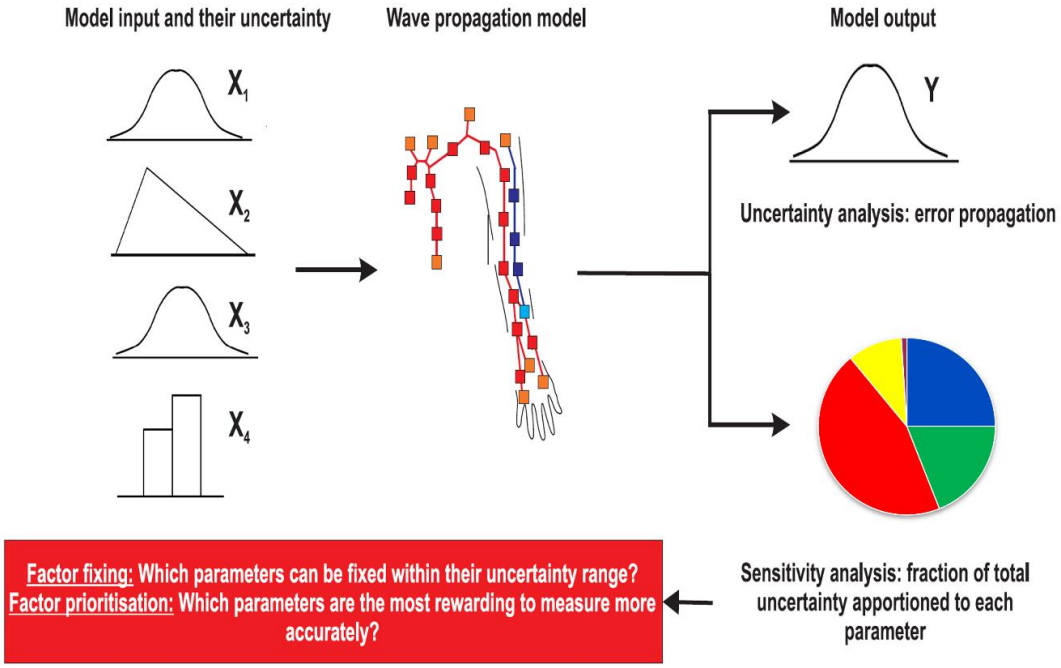

Figure 1: Definition of uncertainty and sensitivity analysis. Based on Saltelli et al.[1,2]

Nonintrusive methods: The algorithm of the (deterministic) model under consideration does not need to be adjusted to be able to perform the sensitivity analysis. In SIMCor we use these types of methods to avoid the need for reprogramming our models when aiming to introduce stochasticity due to model input uncertainties. Nonintrusive methods make our sensitivity analysis tools more widely applicable but unfortunately also requires multiple evaluations of the deterministic model to quantify uncertainties and to identify the most important model input factors. Here the need for fast to evaluate surrogate models comes up again.

Local versus global sensitivity analysis: In local sensitivity analysis only one factor is varied at the time and the subsequent effect on the model response is determined. These types of models might fail as soon as the relation between model response and the input factors is non-monotone, nonlinear and/or non-additive (i.e., interactions are present). In these cases, global sensitivity analyses are needed as these models vary input factors over the input domain simultaneously, hereby also considering interactions. Since the relation between output(s) and input factors is complex, multiple

[1] Saltelli et al., 2019, https://doi.org/10.1016/j.envsoft.2019.01.012
[2] Saltelli et al., 2004, Sensitivity analysis in practice: a guide to assessing scientific models, ISBN 0-470-87093-1

interactions are involved, and often not known *a priori*, in the physiological models used in SIMCor, a global sensitivity analysis is indispensable.

Regionalized sensitivity analysis: This method, also called Monte Carlo filtering, is used to determine which model assumptions, structures or combination of model parameters are responsible for model output realisations in specific areas of the output space (i.e., the realisations that are within a region classified as acceptable according to predefined acceptance criteria). The schematic in Figure 2 depicts the basic idea of this type of sensitivity analysis. An alternative for Monte Carlo filtering is Bayesian analysis.

In the context of SIMCor this approach will be used during virtual cohort generation for defining the filter setting, i.e., the criteria to determine whether a virtually created patient is realistic or not.

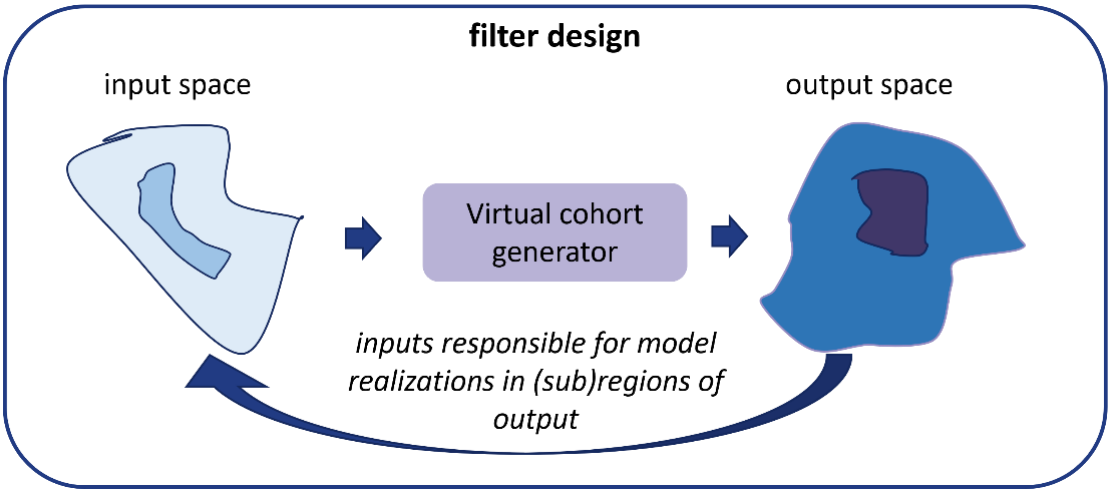

Figure 2: Schematic representation of the regionalized sensitivity analysis that is used to identify selection criteria of the filter.

Envisioned strategy

In SIMCor we will apply ***two different types of sensitivity analysis*** and uncertainty quantification.
The first type is a variance-based technique that is used to identify the model input factors (parameters, assumptions and/or boundary conditions) that are most relevant to measure patient-specifically, and the factors that can be based on population values. This method is indispensable for model personalization, and thus essential during our efforts ***to demonstrate that our physiological models (virtual cohort generators) can accurately mimic patient-specific situations***.
The second type that we will apply is specifically used ***to optimize the filter settings of the filter used during virtual cohort generation***. In fact, here we aim to identify the model input factors that are responsible for model realisations in specific regions of the output space (i.e., relevant regions in the real population distribution). In SIMCor we will use a method based on Monte-Carlo filtering as this nicely fits into our approach for virtual cohort generation. During the project, also Bayesian inference/identification techniques might be considered.

Uncertainty and sensitivity analysis for realistic physiological models

The sensitivity analysis techniques used in this project to assess the model factors (assumptions and/or parameters) are considered the gold standard and based on decomposition of the total output variance[3], i.e., the metric to quantify output uncertainty. These variance-based sensitivity analysis techniques attribute each fraction of the total output variance to individual factors and their uncertainty, or to the interactions between input factors. To quantify these relative contributions both the main and total Sobol sensitivity indices are estimated.

The main Sobol index of an input factor can be interpreted as the expected reduction in total output variance if the exact value of the factor would have been known. This main index is therefore very useful to decide which model input is most relevant to estimate more accurately (factor prioritization), hereby providing guidance to define a measurement protocol for model personalization. The total Sobol sensitivity index of a specific input represents the expected variance that will remain if all other inputs are set on their true value. This index does consider interactions and is typically used to decide which inputs can be set to a constant population value (factor fixing). The connotation of these indices is commonly used in sensitivity analysis research but implicitly assumes that the inputs are statistically independent. Later in this document we present the connotation and estimation of these indices when statistical dependencies (correlations) are present between model inputs.

The Sobol indices introduced above are calculated by integrating the model output over multi-dimensional (sub)spaces spanned by input uncertainties. In nonintrusive methods this is done by strategically sampling the input (sub)space and subsequently evaluating the model for each generated sample. When the computational demand of a single model evaluation increases, the practical applicability of nonintrusive methods decreases. The application of sensitivity analysis is further hindered when the dimensionality of the input space increases (i.e., the “curse-of-dimensionality”). In the remainder of this section, we will therefore briefly explain the methods that we will apply to estimate the Sobol indices in case of computational demanding models and/or models with high numbers of input factors.

[3] Saltelli et al., 2004, Sensitivity analysis in practice: a guide to assessing scientific models, ISBN 0-470-87093-1

Adaptive polynomial chaos expansion method

To estimate the Sobol indices we will use the nonintrusive *adaptive generalized polynomial chaos expansion* (agPCE) method, that was first introduced by Blatman et al.[4], and later applied to computationally expensive cardiovascular models by Quicken et al.[5]

The agPCE method is based on (generalized) polynomial chaos expansion in which the stochastic model output space is spanned by orthogonal polynomials that depend on the stochastic model inputs. When applying the agPCE method, the real model is first evaluated for different samples that are properly distributed throughout the input space. Second, orthogonal polynomials, with increasing polynomial and interaction order, are adaptively added or removed to construct a metamodel (surrogate model) that captures the relation between the model outputs and input samples. As soon as the expansion coefficients of the metamodel are found by means of regression (or spectral projection), the Sobol indices and output variance can be calculated analytically.

Strategies for reducing the required computing resources

Though agPCE using regression is very efficient[4,5], even for computationally demanding models, its practical applicability will decrease for large numbers of inputs (>30) as the maximal required polynomial order and the maximal required interactions order increase. In these cases, more input samples (and thus the number of model evaluations) are needed to create the metamodel.

The decreased applicability of the agPCE due to the "curse-of-dimensionality" could be tackled by first applying Morris screening[6] to eliminate all irrelevant model inputs, and consecutively applying agPCE on the reduced input space. Donders et al.[7] demonstrated that this two-step approach significantly reduced the number of model evaluations when using generalized PCE (i.e., agPCE with a full basis, which means that all basis functions up to the maximal polynomial order are included). Alternatively, we might consider other sparse PCE methods.

Hoeijmakers et al.[8] applied statistical shape modelling to reduce the geometric input space and then conducted UQ and SA using agPCE. Principal component-like analysis techniques might also be considered for reducing parameter input spaces.

Alternative strategies that will be considered in SIMCor to reduce computing resources in case of computationally demanding models (e.g., 3D FSI models) are the development of reduced-order models (0D/1D), reduced-basis models, and/or data-driven emulators (e.g., kernel-based methods). These less computationally demanding models can then be used to generate the output samples needed for agPCE. However, in this case we still need to evaluate the computational demanding models to develop simplified models. In fact, we need to assess for each application whether first developing a simplified model and subsequently using it for sensitivity analysis is more efficient than directly performing sensitivity analysis on the full model.

Different strategies to efficiently conduct sensitivity analysis on the SIMCor applications will be demonstrated in the section that describe our preliminary results.

[4] Blatman et al., 2010, https://doi.org/10.1016/j.ress.2010.06.015
[5] Quicken et al., 2016, https://doi.org/10.1115/1.4034709
[6] Morris et al., 1991, https://doi.org/10.2307/1269043
[7] Donders et al., 2015, https://doi.org/10.1002/cnm.2727
[8] Hoeijmakers et al., 2020, DOI: 10.1002/cnm.3387

Sensitivity analysis to guide filter settings

The *Regionalized Sensitivity Analysis* (RSA) introduced previously is sensitivity in the context of factor mapping, which means that we aim to determine the region of the input space defined by specific output values that fulfill some specifically defined behavior/constraints[9],[10] (e.g., outputs above a certain threshold or not).

In SIMCor, we will use this type of sensitivity analysis to guide the settings of our filter that determine whether a set of model inputs and its corresponding model output realization is included in our virtual cohort or not. In fact, we identify the input region that gives us the desired outputs and decide which inputs we need for filtering, and the corresponding thresholds.

Regionalized sensitivity analysis

To perform RSA, we first need to specify our complete input space. The input space is created based on *a priori* estimates of the input distributions (often uniform marginals are used). Latin Hypercube sampling is used to create a set of input samples that are properly divided throughout the input space (full coverage) and are used for Monte Carlo simulations. Then, a binary classification of the input space is created based on the outputs of the Monte Carlo simulations and specific constraints that define whether the output is in the desired output region or not. This results in a binary set for each input independently: one behavioral set $X_i|B$ where outputs lie within the constraints and one non-behavioral set $X_i|\overline{B}$ otherwise. The distributions of both sets are now tested under the null hypothesis that they are identical using Smirnov two-sample test (two-sided version). If a significant difference between the distributions is found, it can be said that input X_i is of key importance in producing the desired behavior. The sensitivity is quantified by the Kolmogorov-Smirnov distance that is given by:

$$d = sup_y \|F(X_i|B) - F(X_i|\bar{B})\|,$$

which is the supremum of the vertical distance between the cumulative distributions of the behavioral and non-behavioral set.

RSA shows some similarities with the variance-based methods in a sense that they consider the whole range of input factors and that all factors are varied at the same time. In fact, the importance classification of the inputs is related to the main Sobol effects. However, RSA does not search for the (higher order) interactions between inputs, and correlation structures cannot be identified either. Furthermore, the Smirnov test is only a sufficient test if the null hypothesis is rejected (important factor) and is not able to ensure non-importance. These limitations[11], and the fact that higher-order interactions are not considered, imply that further inspection, using for example variance-based methods, is still needed for the factors taken as unimportant by the Smirnov test.

In addition to RSA, we will also consider Bayesian techniques in SIMCor as they can help by identifying the input ranges that result in model realizations in specific outputs regions by analyzing the inverse problem.

[9] Pianosi et al., 2016, DOI: 10.1016/j.envsoft.2016.02.008
[10] Saltelli et al., 2004, Sensitivity analysis in practice: a guide to assessing scientific models, ISBN 0-470-87093-1
[11] Saltelli et al., 2004, Sensitivity analysis in practice: a guide to assessing scientific models, ISBN 0-470-87093-1

Preliminary results aortic valve disease patients

Towards sensitivity analysis of an aortic valve FSI model

The FSI or SSI models to simulate aortic valve stenosis with and without TAVI are still under construction, and/or will be optimized, during SIMCor. The existing models are currently so computationally demanding that we will apply the agPCE method to an in-vitro Mock circulation setup, which is (and will be) used for verification of the in-silico models and allows for fast evaluation of the effect of different input settings on hemodynamic output metrics. It serves as one of the possible surrogate models considered in SIMCor.

The in-vitro approach used in this deliverable already demonstrates the importance of specific inputs on valve-related hemodynamic metrics but also provides insights that can help by better defining the design of future sensitivity analyses on the computationally expensive in-silico models. For example, it can help by reducing the input space by identifying non-important inputs before we conduct the actual sensitivity analyses on the expensive in-silico models.

Study setup

A picture of the mock loop circulation is given in Figure 3. Simply said, the mock loop circulation consists of a pump that mimics the heart, a TAVI device placed to replace the pathological valve, a realistic aortic root and sinus, and a Windkessel model that represents the systemic circulation. The mock loop circulation is setup by consortium partner IIB and represents an integrated part of their state-of-the-art laboratory of device evaluation. The setup can easily be extended so that particle image velocimetry can be performed. However, this is not reported in this document. For more details regarding the circulation setup, we refer to *Deliverable 7.2 - First version of the simulation models (TUE, M9)* on model templates, as well as *Deliverable 8.2 – TAVI model (IIB, M12)* on the TAVI model.

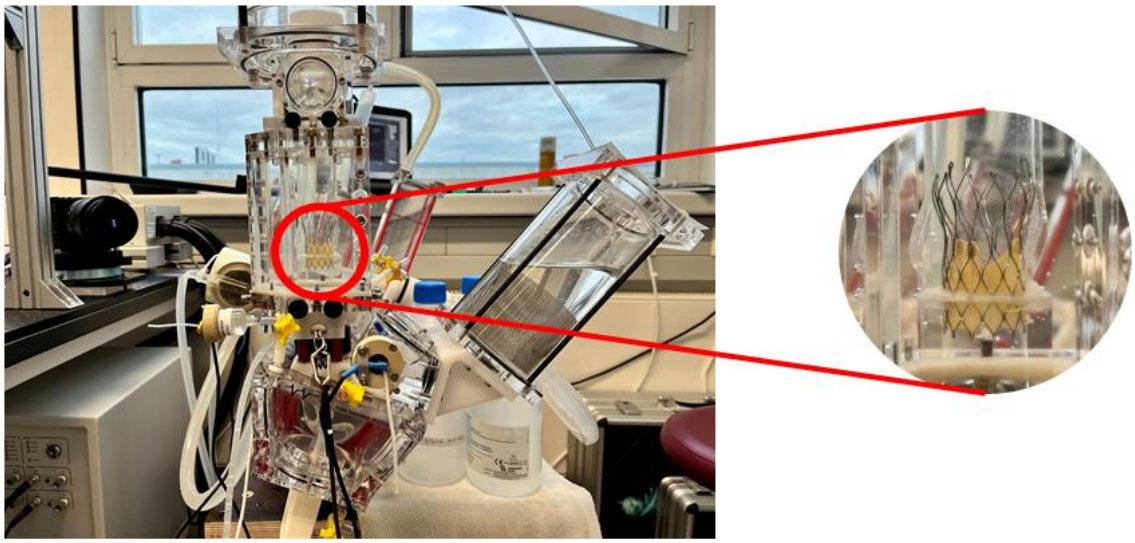

Figure 3: Schematic representation of the experimental setup. Photo provided by the Bioflow lab from the Institute of ImplantTechnology and Biomaterials e.V. (Rostock, Germany).

The input space for our sensitivity analysis is spanned by the uncertainty ranges of the heart rate, aortic mean pressure, percentage systolic time of complete cycle, cardiac output (Table 1), which are all parameters that can be set by the operator. Subsequently, we have randomly sampled the input space by using a low-discrepancy Sobol sequence, i.e., the function *sobolset* in Matlab (MathWorks Version 2021a). Subsequently, we have randomly sampled the input space by using a low-discrepancy

Sobol sequence, i.e., the function sobolset in Matlab (MathWorks Version 2021a). In total 70 samples are generated and the Sobol sequence guarantees that they are properly divided throughout the input space.

Input parameter	Ranges
Heart rate [bpm]	50 – 120
Aortic mean pressure [mmHg]	80 – 120
Percentage systolic time of complete cycle [%]	35 – 75
Cardiac output [l/min]	2 – 10

Table 1: Input ranges for the in vitro analysis.

The 70 input samples generated are used as different input settings for the in-vitro experiments. Since it was impossible to mimic the generated samples exactly in the experiment, we performed the experiments with samples as closely as possible to the sampled ones. The sample values that were really used in the experiments are also fed to our agPCE method during the sensitivity analysis.

For the sensitivity analysis we have defined fourteen different outputs of interest (Table 2). Figure 4 supports the definition of the output metrics.

Output of interest	Definition
TransAortic mean pressure [mmHg]:	Averaged pressure difference between the ventricular and aortic pressure.
TransAortic max pressure [mmHg]:	Maximum pressure difference occurring between the ventricular and aortic pressure.
TransAortic pressure at peak flow [mmHg]:	Pressure gradient between aortic and ventricular pressure during maximum measured forward flow in systole.
Aortic positive pressure time [s]:	Time period during which ventricular pressure exceeds aortic pressure in systole.
Aortic minimum pressure [mmHg]:	Maximum aortic pressure within the entire cycle.
Aortic maximum pressure [mmHg]:	Minimum aortic pressure within the entire cycle.
Pump stroke volume [ml]:	Volume pushed forward by the pump during compression of the ventricular membrane.
Aortic forward flow time [s]:	Time period during which a positive flow volume is measured in systole.
Aortic forward volume [ml]:	Volume ejected during systole in forward flow.
Aortic closing volume [ml]:	Volume that flows back into the ventricle during the closing process.
Aortic leakage volume [ml]:	Volume that flows back into the ventricle transvalvulary or paravalvulary during diastole.
Aortic leakage rate [ml/s]:	Volume per second flowing into the ventricle during diastole.
Aortic regurge fraction [%]:	Percentage of the sum of leakage volume and closure volume in relation to the forward volume.
Aortic orifice area [cm^2]:	Effective orifice area calculated from the following formula: $EOA = \frac{Q_{rms}}{51.6\sqrt{\frac{\Delta p}{\rho}}}$ with $Q_{rms} = \sqrt{\frac{\int_{t1}^{t2} Q(t)^2 dt}{t_2 - t_1}}$

Table 2: Definition of the fourteen outputs of interest.

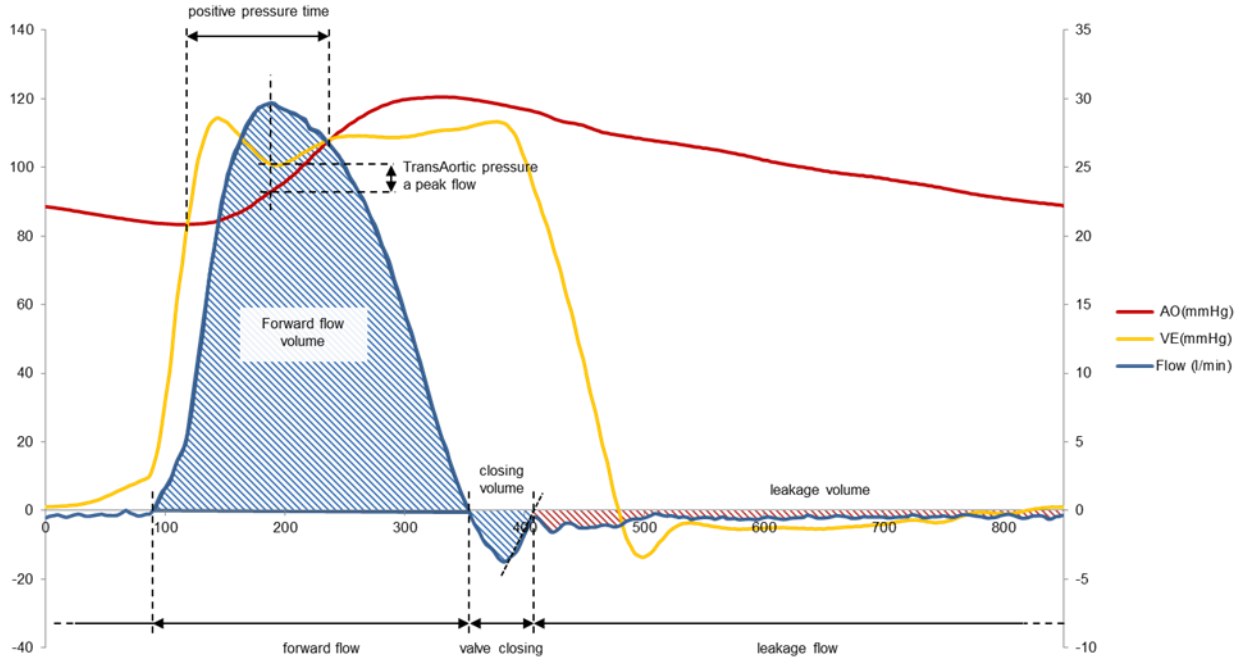

Figure 4: A schematic figure that supports the output definitions in Table 2.

For each output of interest, we have created a metamodel (agPCE) based on the 70 available input samples. The quality of the metamodel is assessed by means of a cross-validation coefficient Q^2, which is preferably as closely as possible to 1.

Results and discussion

For four out of fourteen outputs of interest, it was not possible to fit an accurate meta-model ($Q^2 < 0.85$), because the number of samples was not sufficient. This was the case for the transaortic pressure at peak flow, the aortic closing volume, the aortic leakage volume, and the aortic leakage rate. The sensitivity analysis results for these outputs are not reliable. Therefore, only for the remaining ten outputs of interests the sensitivity analysis results are shown.

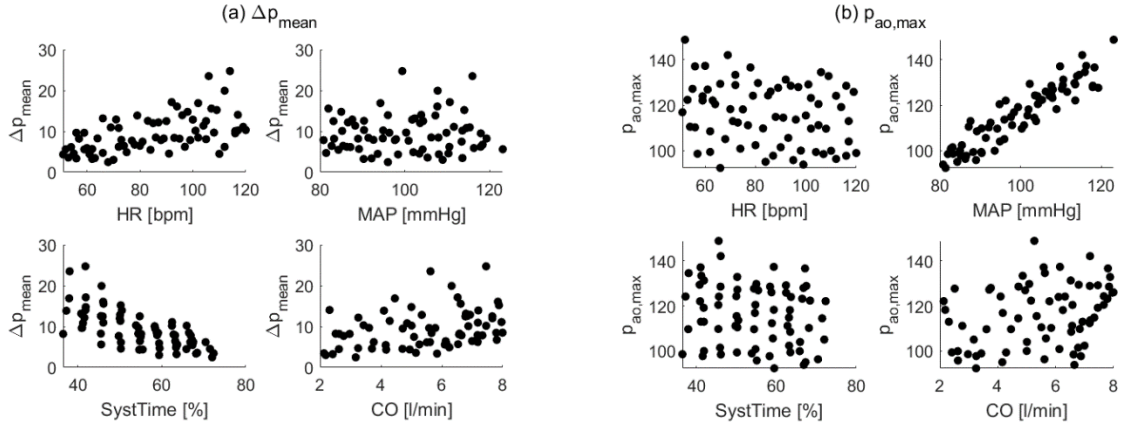

Figure 5: Transaortic mean pressure (Δp_{mean}) (a), and aortic maximum pressure ($p_{ao,max}$) (b) as a function of the 4 inputs heart rate (HR), mean aortic pressure (MAP), percentage systolic time of full cycle (SystTime), and cardiac output (CO).

A typical example of the experimental results for the mean pressure drop across the valve and the maximal aortic pressure as function of the four input parameters, is given in Figure 5. You can observe different trends in the data, (partly) obscured by scattering of points, which results from the influence of other inputs. The agPCE sensitivity analysis is performed on this kind of data.

The main sensitivity indices are visualized in Figure 6. It is visible that the pressure drop across the aortic valve is mainly sensitive to the systolic time duration, and slightly sensitive to heart rate and cardiac output (Figure 6a). These sensitivities correspond with the relations between the input parameters and the mean pressure drop as visualized in Figure 5a. For the transaortic mean pressure there is a negative relation with the systolic time duration (Figure 5a, bottom left). This relation is caused by the fact that the pressure difference between the left ventricle and the aorta is decreased during the systolic phase. As a result, the mean pressure drop decreases with increasing systolic time. A slight dependency of the mean pressure drop on the heart rate (top left) and the cardiac output (bottom right) is visible in Figure 5a as well. The high sensitivity of the minimum and maximum aortic pressure to the mean arterial pressure, is confirmed by the strong relation that is visible in Figure 4b (top right).

The pump and forward flow volume are only sensitive to heart rate and cardiac output (Figure 6c), which makes sense, because stroke volume is equal to cardiac output divided by heart rate. Furthermore, the positive pressure time, and forward flow time are only sensitive to heart rate and systolic time duration (Figure 6b). Finally, Figure 6d shows a high sensitivity of the regurgitation fraction and the aortic orifice area to the cardiac output. This sensitivity can be explained by the form of the definitions used for regurgitation fraction, and the aortic orifice area, that both strongly depend on cardiac output.

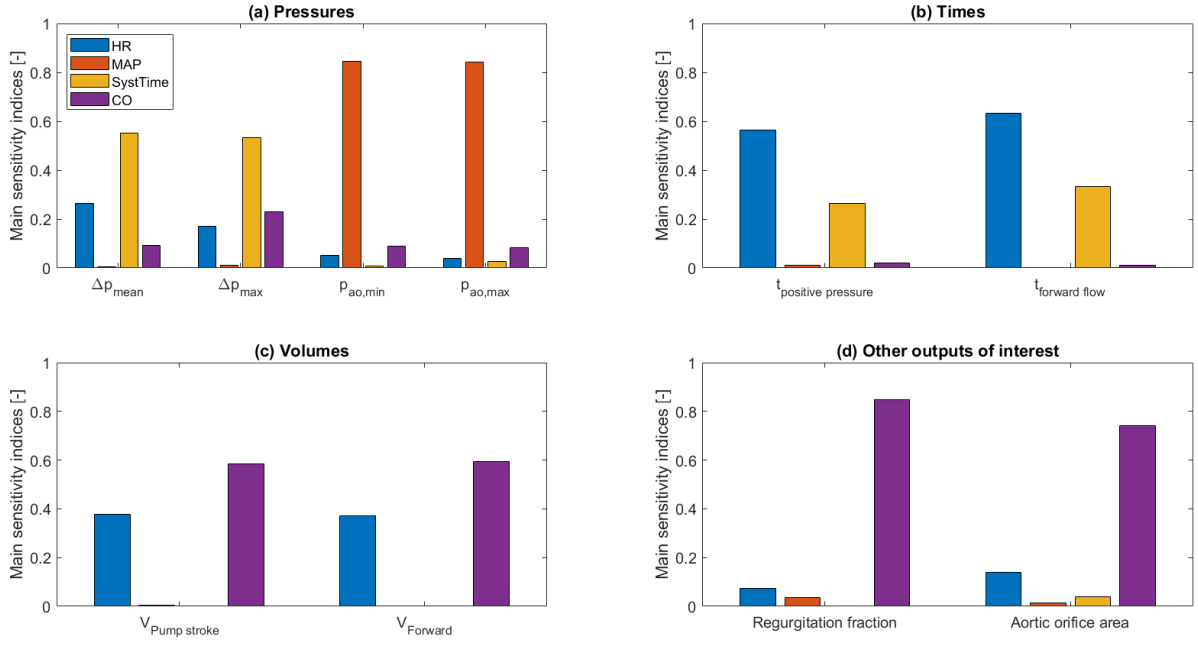

Figure 6: Main sensitivity indices of multiple outputs of interest for the four different input parameters heart rate (HR), mean aortic pressure (MAP), percentage systolic time of complete cycle (SystTime), and cardiac output (CO): (a) Pressures: transaortic mean pressure (Δp_{mean}), transaortic maximum pressure (Δp_{max}), aortic minimum pressure ($p_{ao,min}$), and aortic maximum pressure ($p_{ao,max}$). (b) Times: positive aortic pressure time ($t_{positive\ pressure}$), and aortic forward flow time $t_{forward\ flow}$). (c) Volumes: pump stroke volume ($V_{Pump\ stroke}$), and aortic forward volume ($V_{forward}$). (d) Other outputs of interest: Regurgitation fraction, and aortic orifice area.

In Figure 7 the differences between the main and total sensitivity analysis are shown. The difference between the main and total index quantifies the contribution of a specific input to the total output variance via interactions with other inputs. The percentage of systolic time of complete cycle and the heart rate are significantly involved in interactions with other inputs when considering the outputs transaortic mean pressure drop (respectively 7% and 8%) and the positive aortic pressure time (both about 10%). The cardiac output has also a significant interacting effect on the positive aortic pressure

time (about 7%). All other visible interactions are smaller than 5%. Though the effect of interactions needs to be considered, the overall effect on the outputs is relatively small.

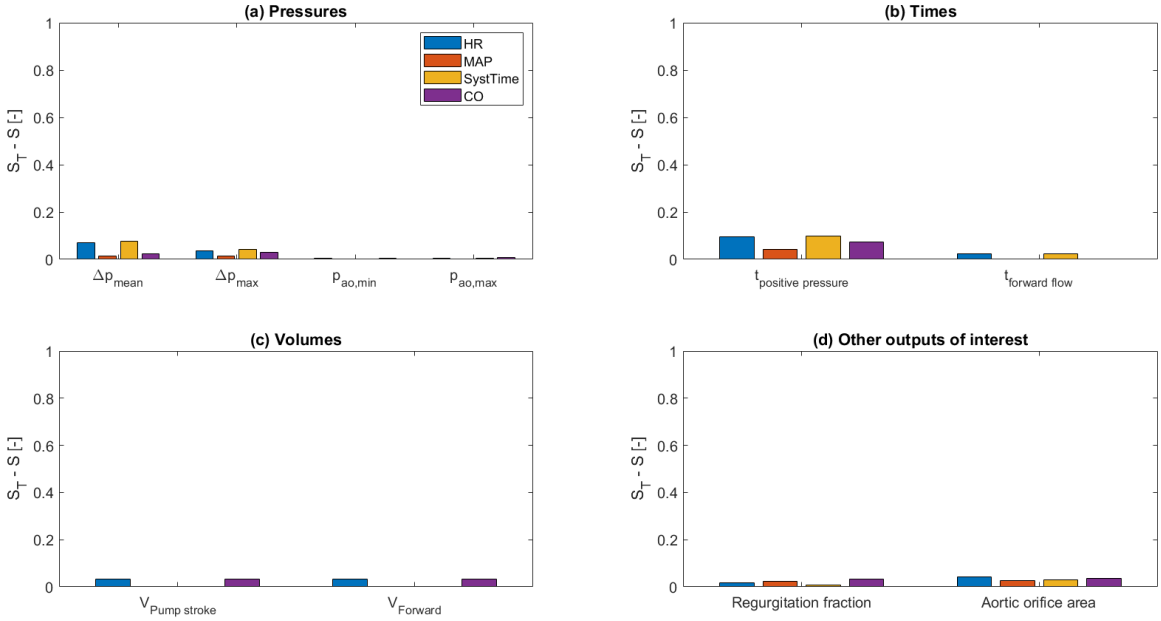

Figure 7: The differences between the main and total sensitivity indices, which are representative for the contribution of inputs on the output variance via interactions with other inputs.

This sensitivity analysis provides insight towards which parameters can be set to a population-based constant (non-important on itself and not via interactions), and which parameters must be set to a patient specific value, to obtain precise model simulation results of the aortic valve with TAVI. More specifically, the main indices can be used to rank which model inputs are most rewarding to measure as accurate as reasonably possible. Outputs that are important for TAVI are for example the regurgitation fraction, and the pressure drop across the aortic valve, because they are both related to paravalvular leakage. To be able to obtain accurate values for the regurgitation fraction, the uncertainty in the cardiac output should be as small as possible. For the pressure drop, the mean arterial pressure could be set to a constant, but the patient specific heart rate, cardiac output, and especially the systolic time duration, should be known very accurately.

Sensitivity analysis for filter design

In this section we will present the preliminary results of the RSA technique applied to a model of aortic valve stenosis patients, and its corresponding input space, that is used for virtual cohort generation. The model on which we apply the sensitivity analysis is an emulator of a computationally demanding CFD model that can estimate the peak systolic pressure drop across an aortic valve stenosis, and was previously described in *Deliverable 7.3 - First version of the definition of the input space (TUE, M12)* and the publication of Hoeijmakers et al. The inputs of the models are the peak systolic aortic flow, a scaling parameter and five shape mode coefficients of a statistical shape model (i.e., geometric parameters), resulting in a seven-dimensional input space.

Study setup

For the sensitivity analysis in this deliverable, we only focused on the geometric subspace of the full 7D input space. Subsequently, we have generated multiple input samples from this input space by means of Latin Hypercube sampling. Thereafter, we used the input samples to construct the corresponding aortic valve geometries, and for these geometries we quantified the cross-sectional areas of the *left ventricular outflow tract* (LVOT), the *aortic valve opening* (AV), the *ascending aorta diameter* (AA), the *sinus* (SIN), the *sinotubular junction* (STJ) and the *annulus* (ANU). These geometric metrics constitute the input space used for the regionalized sensitivity analysis. The input ranges defining the boundaries of the input space are given in Table 3.

Input parameter	Ranges
LVOT [cm^2]	1.58 – 5.94
AV [cm^2]	0.0 – 4.59
AA [cm^2]	2.23 – 10.89
SIN [cm^2]	3.33 – 11.56
STJ [cm^2]	2.19 – 10.41
ANU [cm^2]	2.12 – 7.13

Table 3: Input ranges of the geometric inputs used for the sensitivity analysis.

To demonstrate the feasibility of the RSA in identifying the inputs that are mostly responsible for output realizations in specific regions of the output space, we have introduced a threshold for the peak systolic pressure drop across the aortic valve stenosis. This threshold was set to 300 mmHg, and all output realizations larger than this threshold are considered non-behavioral (i.e., non-physiological outputs).

Results and discussion

Figure 8 shows the scatter plots and *cumulative distribution functions* (CDF) of two different inputs, i.e., the areas of the LVOT and the AV. Figure 8a and 8b show the differences between the behavioral and non-behavioral distributions based on the chosen threshold. As can be seen, in Figure 8a there is no real difference in spread of the behavioral and non-behavioral points, resulting in the CDFs in Figure 8c. Here it can be seen that both the behavioral and non-behavioral distribution are almost equal. On the contrary, when looking at Figure 8b a nonlinear, monotone decreasing relation can be observed. Because of this distribution, a second observation can be made which is that the spread of the non-behavioral points is a lot smaller than the spread of the behavioral points. As a result, there also is a bigger difference between the CDFs of the behavioral and non-behavioral sets (Figure 8d).

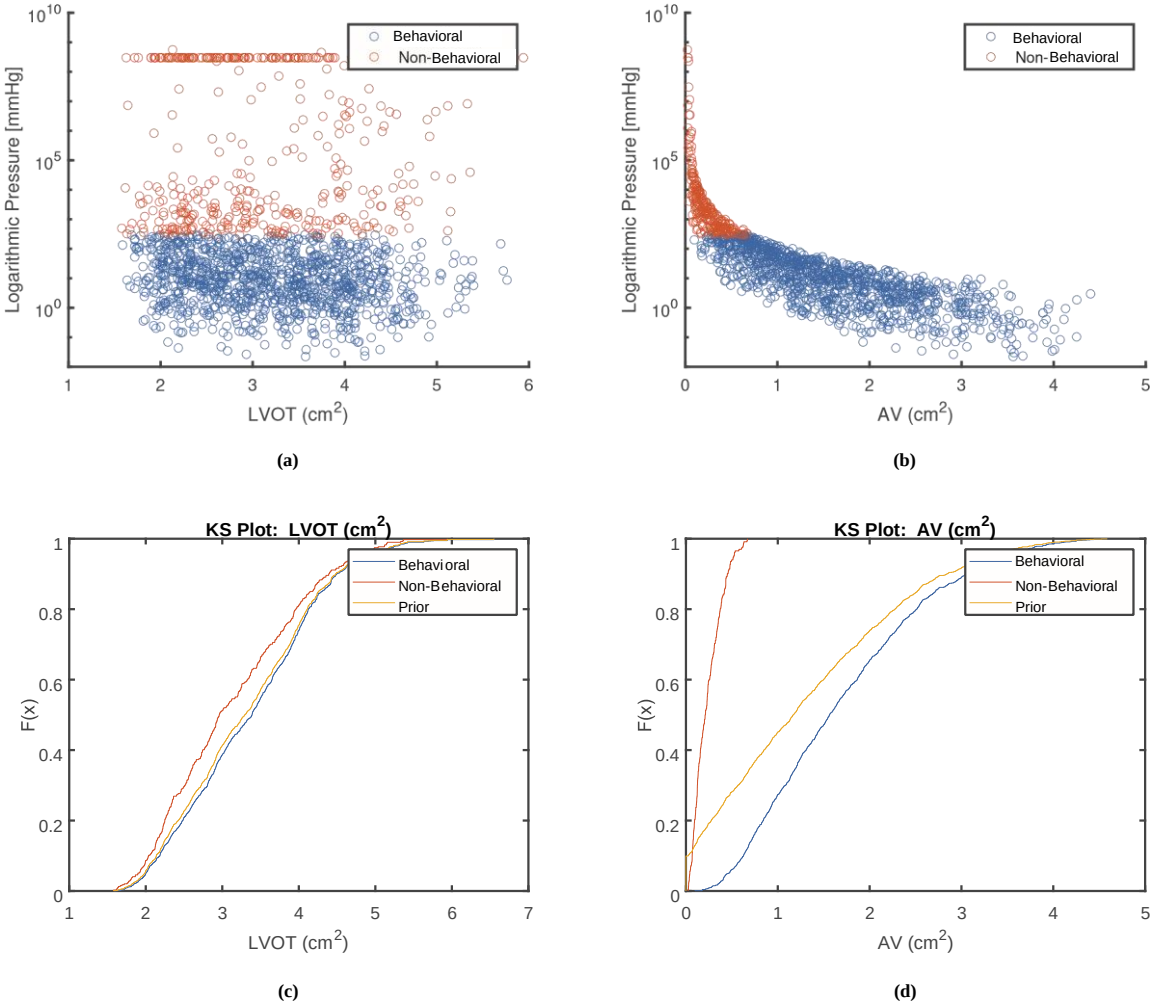

Figure 8: The top figures represent the scatterplot where input is plotted against the logarithmic output of the pressure drop. Where the behavioral points are in blue, and the non-behavioral points are in orange. The bottom figures show the cumulative distribution function of the behavioral and non-behavioral samples, the yellow line shows the cumulative distribution of the full distribution, prior to splitting the data into two groups.

The observations made in the previous figure can be quantified by means of the Kolmogorov-Smirnov distance and the p-value after statistical hypothesis testing. The results in Figure 9 show that the LVOT AA, ANU, SIN and STJ all have relatively low Kolmogorov-Smirnov distances (< 0.2), whereas the AV has a large distance (0.9). The LVOT, AV, ANU and SIN have low p-values that indicate that there is sufficient evidence to reject the null hypothesis, i.e., the inputs do have a significant effect on producing desired (physiological) behavior. For the other two inputs the statistical evidence of rejecting the null hypothesis is insufficient.

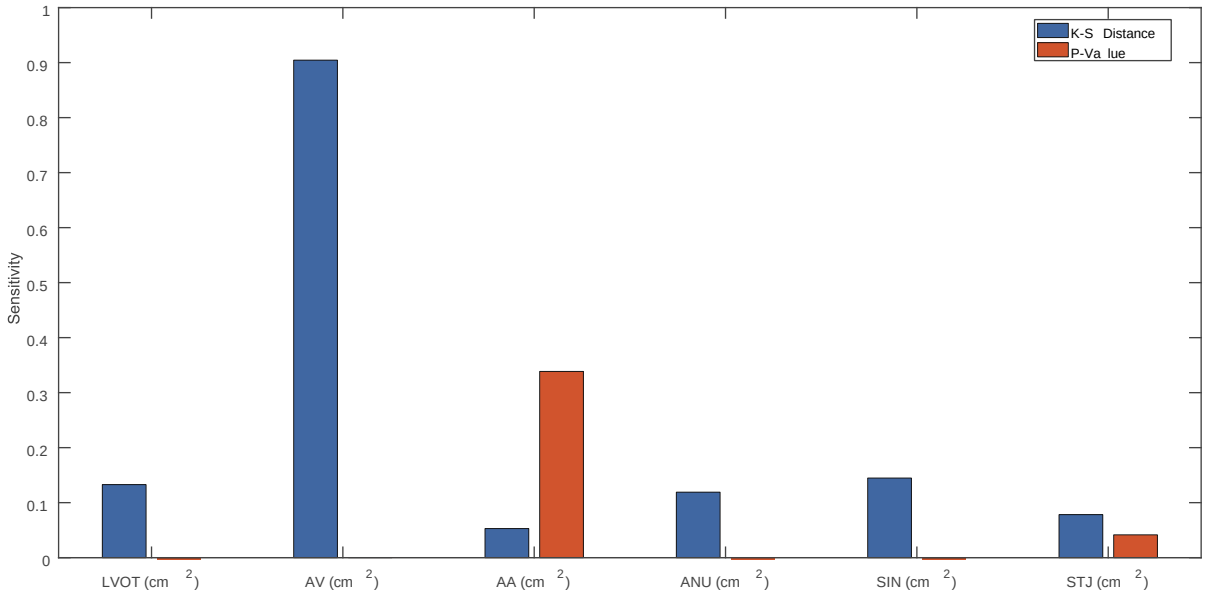

Figure 9: The Kolmogorov-Smirnov (K-S) distances and the p-values of the Smirnov test.

An important remark to be made is that the ranking of the inputs was found to be affected by the number of of data samples that were used. This could be due to difference in the number of samples in the behavioral or non-behavioral sets. To prevent this from happening input sample set should be sufficient large to ensure enough statistical power and accurate input ranking.

Preliminary results for heart failure patients

Sensitivity analysis of a pulmonary artery CFD model

In this section we will apply the agPCE method on a 3D CFD model of the main, left and right pulmonary arteries. Three-element Windkessel models, mimicking the distal vasculatures, are coupled at the outlets of the *left pulmonary artery* (LPA) and the *right pulmonary artery* (RPA). At the inlet of the *main pulmonary artery* (MPA) a typical inlet flow waveform is applied by means of a transient plug velocity profile. The 3D computational domain consists, after mesh convergence analysis, of 1.3 million tetrahedral volumetric mesh elements with an average quality of 0.68. Blood flow was considered as a laminar, incompressible, and Newtonian fluid. Dynamic blood viscosity and density are set to 1065 kg/m^3 and $3.5 \cdot 10^{-3}\ Pa \cdot s$, respectively. The 3D transient pressure and velocity fields within the computational domain are calculated by using COMSOL Multiphysics.

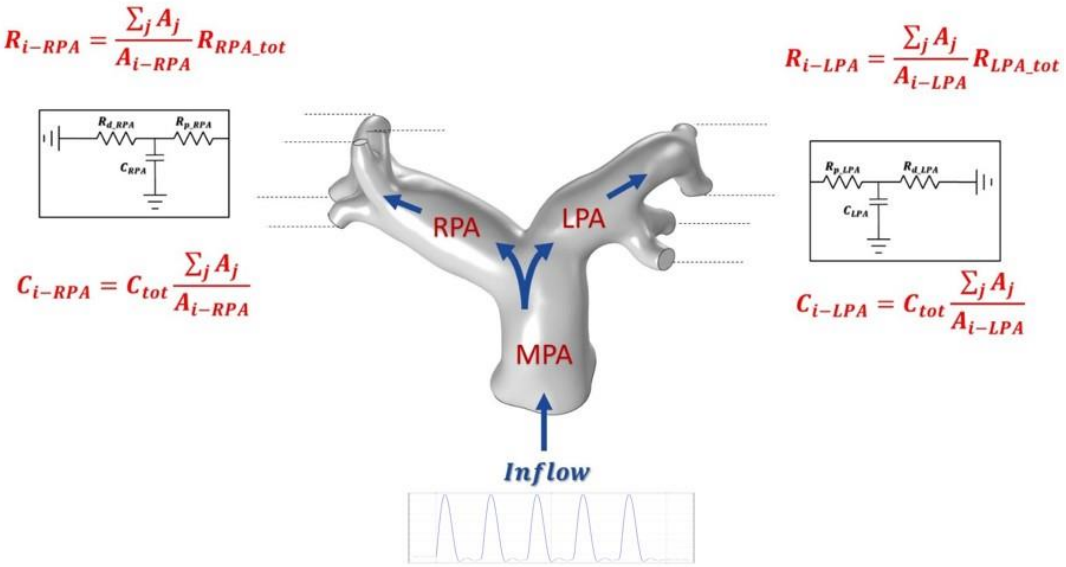

Figure 10: The differences between the main and total sensitivity indices, which are representative for the contribution of inputs on the output variance via interactions with other inputs.

The input space for the sensitivity analysis is spanned by four uncertain inputs: stroke volume, heart rate, flow ratio (RPA/LPA), and the total distal arterial compliance. The input ranges are defined as presented in Table 4. The input is subsequently sampled within these physiological ranges using the low-discrepancy Sobol sequence via the built-in Matlab function *sobolset (MathWorks Version 2021a)*. Based on an *a priori* estimation a database of 30 samples is created.

Input parameter	Ranges
Q_{RPA} to Q_{LPA} ratio [-]	45 – 65 [12]
Stroke Volume [ml]	50 – 150 [13]
Total Compliance [ml/mmHg]	1 – 4 [14]
Heart Rate [bpm]	60 -120 [15]

Table 4: Input ranges for the sensitivity analysis.

The CFD model is now executed for all thirty input samples and the model outputs of interest are derived from the simulations. *Mean pulmonary artery pressure* (MPAP) and the *mean time-averaged*

[12] Wehrum et al., 2016, DOI: 10.1186/s12968-016-0252-3
[13] Van Ooijen et al., 2012, DOI: 10.1148/rg.322115058
[14] Guigui et al., 2020, DOI: 10.21037/jtd.2020.02.20
[15] Jose et al., 1970, DOI: 10.1093/cvr/4.2.160

MPAP

wall shear stress (MTAWSS) are our outputs of interest. By constructing and testing a large set of meta-models, the meta-model with the highest Q^2 was selected as final model for each output of interest. The metamodel with $Q^2 = 0.9995$ is used for the analysis. Both of our outputs of interest are sensitive to stroke volume (main index of respectively 68% for MPAP and 62% for MTWSS) and heart rate (main index of respectively 30% for MPAP and 34% for MTWSS). It seems that there is not any meaningful sensitivity from total compliance and flow distribution for both MPAP and MTAWSS (main indices < 0.1%). Similar ranking is found for the total sensitivity indices for MPAP (stroke volume: 70%, heart rate: 32%) and MTWSS (stroke volume: 65%, heart rate: 38%). For both outputs the variance contributions of interactions are small (<4%).

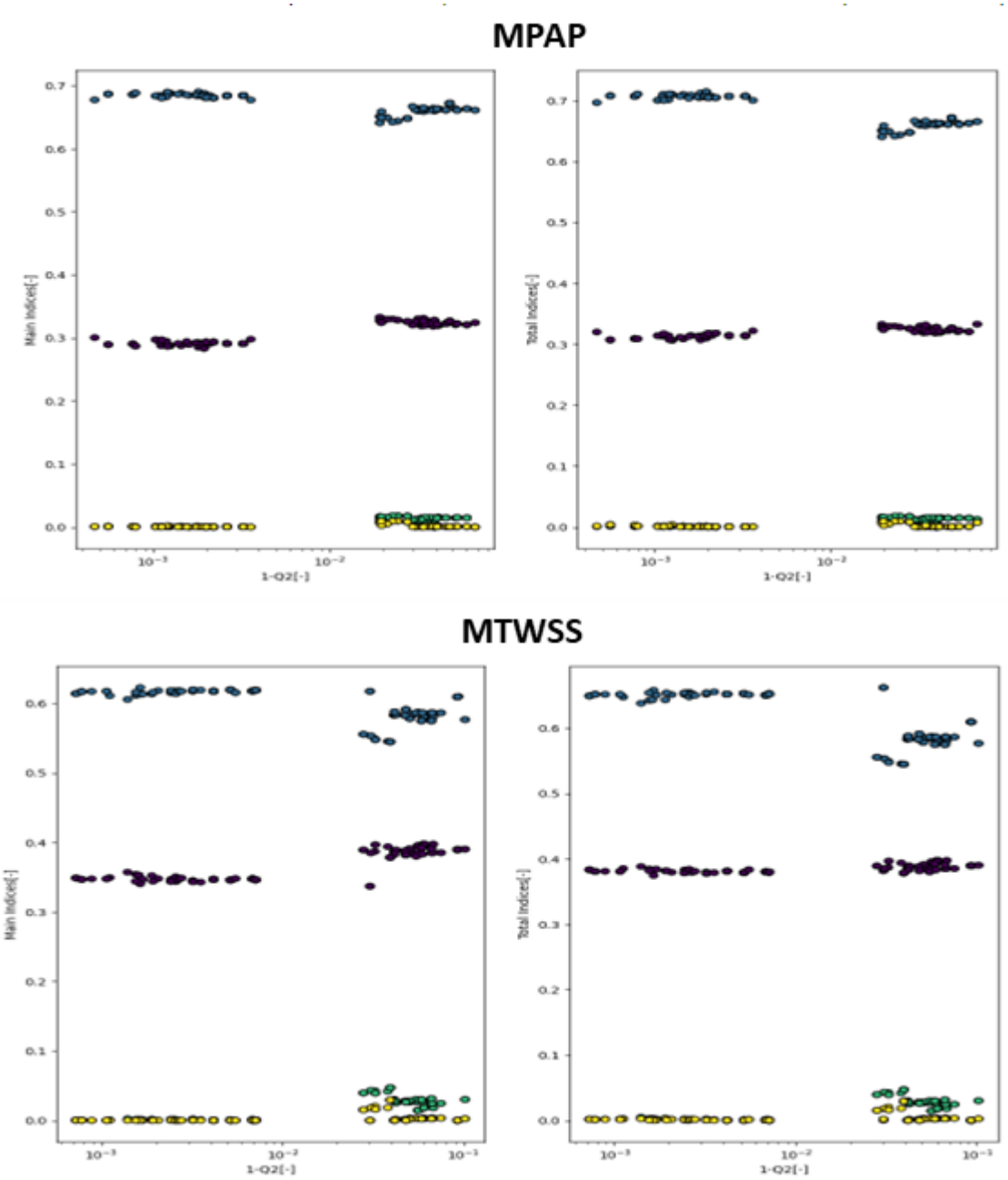

Figure 11: The main and total sensitivity indices as function of the quality of the polynomial chaos expansion for the MPAP (top) and the MTWSS (bottom). Blue dots are for stroke volume, purple for heart rate, green for total compliance and yellow for the flow distribution.

Two-step approach for sensitivity analysis using a surrogate model

The model for our SIMCor application of heart failure patients consists of a 3D domain of the pulmonary arteries (region of interest) coupled to a closed-loop lumped parameter model of both the pulmonary and systemic circulation (Figure 12, left). The lumped parameter can generate proper boundary conditions for the 3D region of interest in pathological heart conditions, both before and after PAPS implantation. Though the boundary conditions are more realistic and automatically respond to changes in pre- and afterload (PAPS insertion), the number of model parameters significantly increases. The latter will make the sensitivity analysis ("curse-of-dimensionality") almost impossible as it requires an enormous number of CFD evaluations (>1000), and thus computing resources, to feed the agPCE.

Therefore, we envision another, ***two-step strategy***. In the ***first step*** a reduced-order lumped parameter (0D) model that mimics the (nonlinear) pressure-flow relation (impedance) of the 3D region of interest will be derived and integrated in the closed-loop circulation model (Figure 12, right). Subsequently, the inputs of the now full 0D model will be varied and the model will be evaluated (closely to real-time) for all input samples. This leads to a set of pressure and flow waveforms at the inlet and outlets of the pulmonary arteries. Thereafter, the agPCE method can be applied to identify the inputs that have a significant influence on these in- and outlet conditions. Our hypothesis is that this first step of the sensitivity analysis will significantly reduce the total number of inputs, i.e., the parameter input space will be reduced. In the ***second step***, we will then apply sensitivity analysis using agPCE on the 3D/0D model but not by exploring the reduced input space.

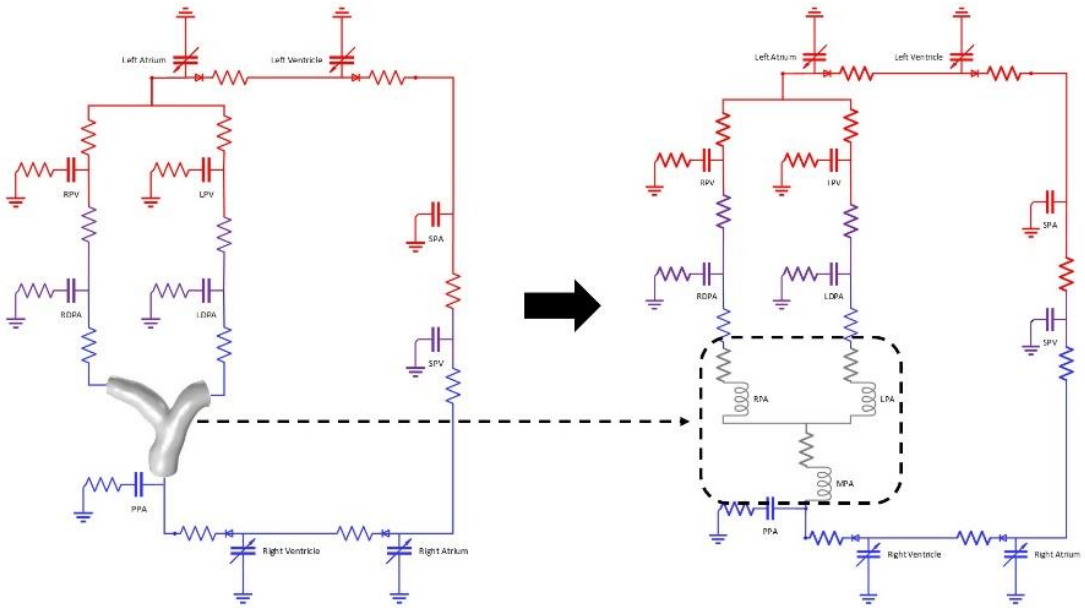

Figure 12: The closed-loop lumped parameter model of the systemic and pulmonary circulations.

In this deliverable we will present our first approach to derive a lumped parameter model that accurately represents the impedance of the rigid 3D domain (in future a moving domain may be considered). The MPA, RPA and LPA are each modelled with a resistance and an inertance. The numerical values are first estimated using respectively the mathematical expressions of a Poiseuille resistance and the inertance, fed by geometric information, blood density and dynamic viscosity. Thereafter, they are further optimized based on CFD simulation results with different inlet flows. Below you can see the preliminary results of the lumped parameter model for different pressure drops from the inlet to different outlets as function of time. These results show the feasibility of deriving an accurate lumped model for the 3D pulmonary arteries. In future work we will also explore another

approach that was introduced by Mirramezani et al.[16] and showed reasonably accurate results for different cardiovascular applications purely based on geometric information and blood properties.

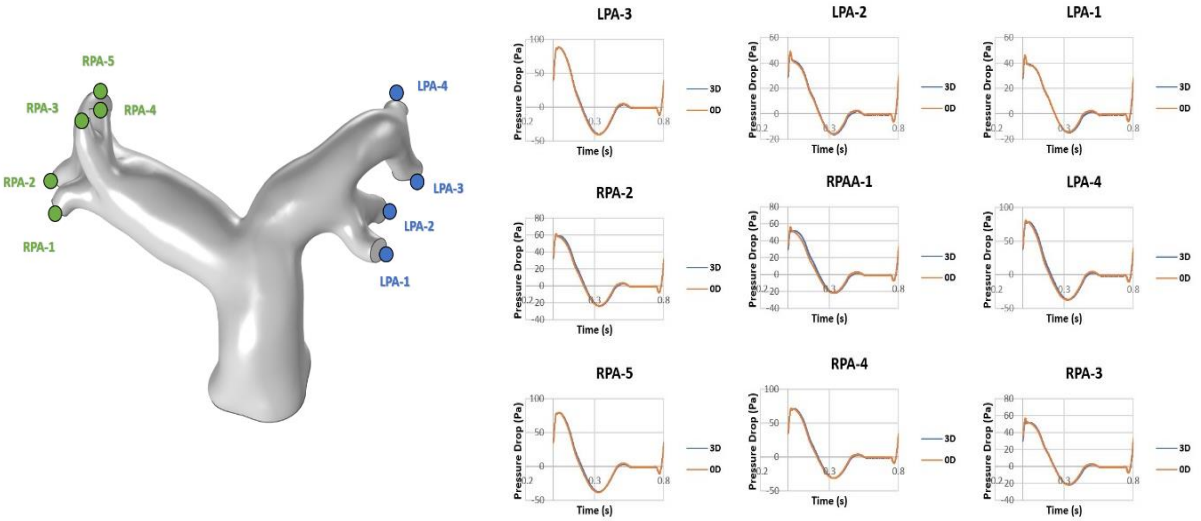

Figure 13: Simulated pressure drops, using both the 3D and 0D model, from the inlet to different outlets.

[16] Mirramezani et al., DOI: 10.1007/s10439-020-02545-6

Future work

In future project activities, we will also use sensitivity analysis techniques that are able to consider statistical dependencies between model inputs when the physiological model under investigation advocates for this and the statistically dependencies are known. If the dependencies are not exactly known, we will evaluate different correlations to examine how possible correlations will affect our conclusions regarding input parameterization and fixing. These new sensitivity analysis techniques will also provide us information whether future efforts to find correlation structures are rewarding or not.

In the next subsection we will present our current implementation of a sensitivity analysis technique that considers statistical dependencies between model inputs and that was introduced by Li et al.[17] Thereafter, we will briefly explain how we are planning to apply our sensitivity tools (also the correlated ones) in future project deliverables.

Sensitivity analysis with statistical dependent input parameters

Background and methodology

Both the connotation and estimation of the Sobol sensitivity indices described above are derived under the assumption of statistically independent model inputs. In case of statistically dependent model inputs the connotation[18] of these indices change and, in addition, we need to adapt the way these indices are calculated.

The main Sobol sensitivity index in the case of statistical dependent model inputs captures the total correlated contribution of the input to the output variance, i.e., the summation of the variance contribution solely caused by the input itself and the variance contribution of all correlations the input is involved (both with interaction terms and with individual other inputs).

The total sensitivity index is the total uncorrelated contribution and considers no contributions due to correlations but solely variance contributions due to the input itself and the interactions of this input with other parameters.

To estimate the multi-dimensional integrals that define the sensitivity indices, we have thus adopted the approach of Li et al. [18] and implemented this in MATLAB (MathWorks Version 2021a). Thereafter, we have first applied it to benchmark problems, for which analytical estimates of the indices exists and which were also used by Li et al.[18], to verify our implementation. Thereafter, we have applied the method to a 1D model that is able to simulate pressure and flow wave propagation throughout the cardiovascular system.

Application to simple non-linear and polynomial function

The first benchmark problem is the simple non-linear function defined as:

$$Y = X_1 X_2 + X_3 X_4.$$

It is assumed that X_1 and X_2 are correlated with the correlation coefficient $\rho_{13} = 0.3$ and that X_3 and X_4 are correlated with the correlation coefficient $\rho_{34} = -0.3$. The computed analytical variance contributions compared to the analytically computed variance contributions are shown in Figure 14.

[17] Li et al., 2017, http://dx.doi.org/10.1016/j.ast.2016.12.003
[18] Li et al., 2017, http://dx.doi.org/10.1016/j.ast.2016.12.003

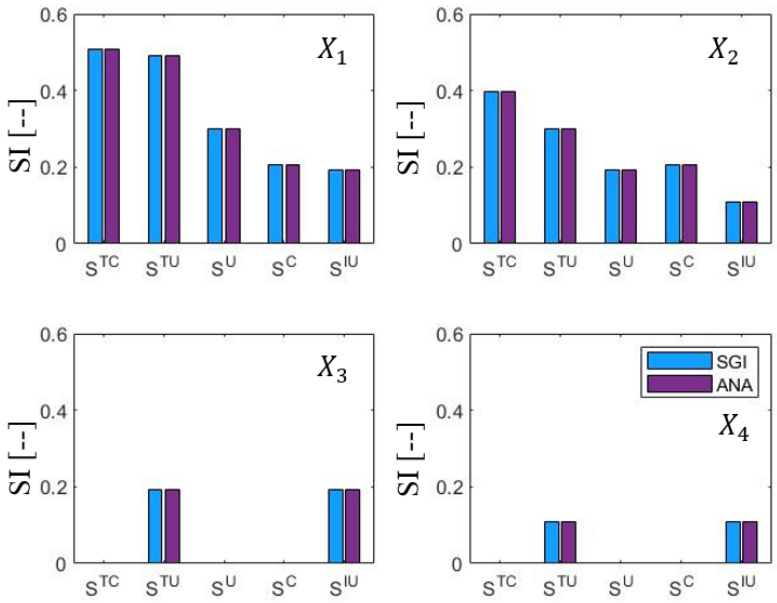

Figure 14: Li et al. based and analytical estimates of the variance contributions for the non-linear model.

As can be seen, the computed sensitivity indices agree with their analytically derived counterparts. These results agree with the implementation of Li et al. [19] as well. The second benchmark problem is the simple polynomial defined as:

$$Y = 5 + 8X_1 + X_2^2.$$

The inputs were correlated by a coefficient of $\rho_{12} = 0.5$. The computed analytical variance contributions compared to the analytically computed variance contributions again agree and are shown in Figure 15.

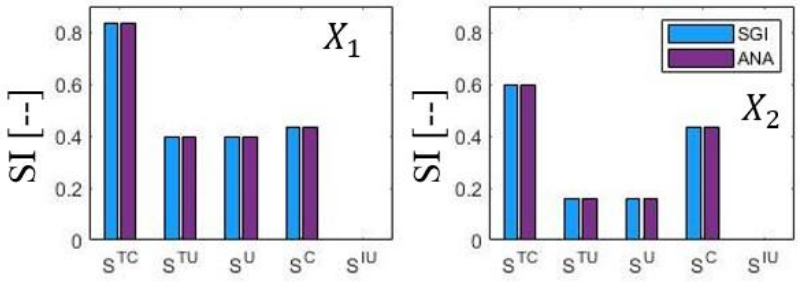

Figure 15: Li et al. based and analytical estimates of the variance contributions for the polynomial model.

Application to Ishigami functions with different parameterizations

The third benchmark problem are the Ishigami functions. The first Ishigami function is defined as:

$$Y = \sin X_1 + a \sin^2 X_2 + bX_3^4 \sin X_1.$$

All input variables are uniformly distributed in the interval $[-\pi, \pi]$. It is assumed that X_1 and X_3 are correlated with the correlation coefficient $\rho_{13} = 0.4$. For the uniformly distributed input variables, the zeros of the Gauss-Legendre polynomials are used as one-dimensional quadrature points. A Gaussian copula is used to transform the original problem to the case of the correlated normal one.

[19] Li et al., 2017, http://dx.doi.org/10.1016/j.ast.2016.12.003

The computed variance contributions are shown in Figure 16.

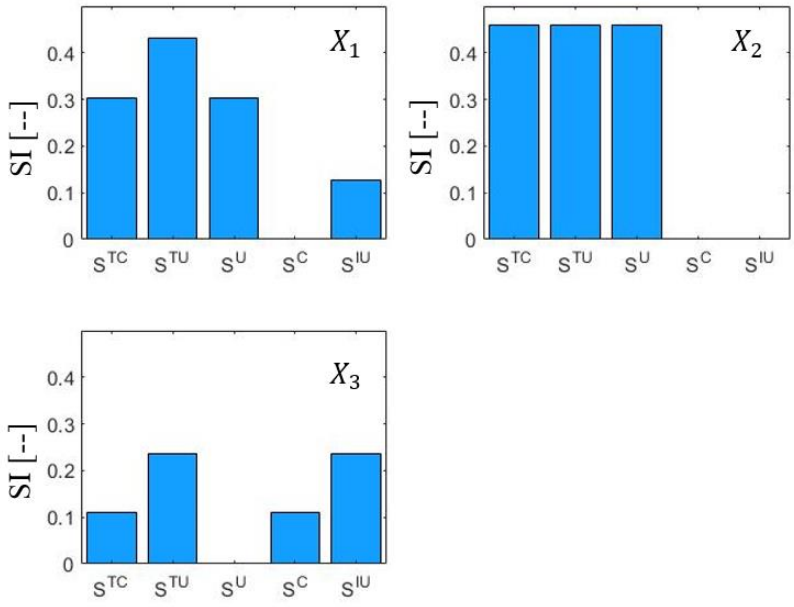

Figure 16: Numerical estimates of the various variance contributions for the input variables of the Ishigami function.

They are like the SGI computed variance contributions found by Li et al. Furthermore, Li et al. also applied their method to the following two forms of the Ishigami function:

$$Y_1 = \sin X_1 + a \sin^2 X_2 + bX_3^4 X_1^4$$

and

$$Y_2 = \sin X_1 + a \sin^2 X_2 + \sin^2 X_3.$$

For both forms, again X_1 and X_3 are correlated with the correlation coefficient $\rho_{13} = 0.4$. The computed estimates of these Ishigami functions are given in Table 5.

Y_1	S_i^{TC}	S_i^{TU}	S_i^{U}	S_i^{C}	S_i^{IU}
X_1	0.3812	0.6184	0.1752	0.2060	0.4432
X_2	0.0004	0.0004	0.0004	0.0000	-0.0000
X_3	0.3812	0.6184	0.1752	0.2060	0.4432
Y_2	S_i^{TC}	S_i^{TU}	S_i^{U}	S_i^{C}	S_i^{IU}
X_1	0.0741	0.0689	0.0689	0.0053	0.0000
X_2	0.9074	0.9074	0.9074	0.0000	0.0000
X_3	0.0237	0.0185	0.0184	0.0053	0.0000

Table 5: Estimates of the various variance contributions for the two forms of the Ishigami functions.

Again, comparing these results to the results found by Li et al., it was found that they correspond very well with one another. The largest difference found between the indices is a difference of 0.015, which is considered negligible when it comes to assessing the sensitivity.

Application to a pulse wave propagation model

The 1D pulse wave propagation model on which we will apply our sensitivity analysis was already presented in *Deliverable 7.2 - First version of the simulation models (TUE, M9)*. However, for

readability we will summarize the basic components of the model before we move on to the sensitivity analysis.

The 1D model consists of serially connected arterial elements that form the ADAN56 vascular tree. Each element represents the local relation between pressure and flow via mass conservation, momentum balance and a constitutive law to capture vessel mechanics. At the end of truncated vessels three-element Windkessel models are placed to mimic the distal vasculature. On the first arterial node (aorta) a time-dependent flow waveform is prescribed. All inputs of the elements and boundary conditions (inflow and Windkessels) are provided in the supplementary material of Boileau et al.[20], in which our numerical implementation was benchmarked against other numerical schemes. However, for the analysis in this deliverable we have used another velocity profile to express the wall shear stress and the advection term in the momentum balance in terms of pressure and flow, because this velocity[21] better captures the physics than the profile used in Boileau et al.

To conduct the sensitivity analysis, we have defined 23 model inputs (Table 6). To avoid unrealistic combinations of model inputs, we have grouped different vessels together and varied their inputs (Young's modulus, radii and length). Also, the Windkessel parameters are grouped. A similar approach was taken by Melis et al.[22] who performed a sensitivity analysis on a 1D model by using Gaussian process emulators, and by assuming statistically independencies between the inputs. We also adopted the input uncertainty ranges of Melis et al., expect for the Windkessel compliances that are chosen to be 30% instead of 50%. The complete input space used in this study is given in Table 6 (for now still assuming no correlations/statistical dependencies).

Input parameter	Ranges
E_{aorta}	*-20% – 20%*
E_{organs}	*-20% – 20%*
$E_{upper\ limbs}$	*-20% – 20%*
E_{neck}	*-20% – 20%*
$E_{lower\ limbs}$	*-20% – 20%*
l_{aorta}	*-10% – 10%*
l_{organs}	*-10% – 10%*
$l_{upper\ limbs}$	*-10% – 10%*
l_{neck}	*-10% – 10%*
$l_{lower\ limbs}$	*-10% – 10%*
$r0_{aorta}$	*-10% – 10%*
$r0_{organs}$	*-10% – 10%*
$r0_{upper\ limbs}$	*-10% – 10%*
$r0_{neck}$	*-10% – 10%*
$r0_{lower\ limbs}$	*-10% – 10%*
R_{organs}	*-25% – 25%*
$R_{upper\ limbs}$	*-25% – 25%*
R_{neck}	*-25% – 25%*
$R_{lower\ limbs}$	*-25% – 25%*
C_{organs}	*-30% – 30%*
$C_{upper\ limbs}$	*-30% – 30%*
C_{neck}	*-30% – 30%*
$C_{lower\ limbs}$	*-30% – 30%*

Table 6: Inputs and ranges used during the sensitivity analysis of the pulse wave propagation model.

Currently, correlations are unknown to us so we will vary them ourselves to find out the effects of the correlations on the computed variance contributions/sensitivity indices.

[20] Boileau et al., 2015, DOI: 10.1002/cnm.2732
[21] Bessems et al., 2007, DOI:10.1017/S0022112007005344
[22] Melis et al., 2017, DOI: 10.1002/cnm.2882

To quickly compute the variance contribution of the PWPM, a two-step approach is used. First, a surrogate model of the PWPM is created by making use of a Vectorial Kernel Orthogonal Greedy Algorithm (VKOGA) method[23,24]. This VKOGA method allows for the creation of a kernel function based on a finite set of inputs and outputs generated with the PWPM. This kernel function in turn allows us to quickly relate input variables to a certain output.

The second step is performing the SGI sensitivity analysis using the kernel function. No correlations were added to be able to compare the results obtained by the two-step approach with the results obtained by the uncorrelated agPCE SA method. For both methods, the variance contributions to two certain outputs were derived, namely the systolic and diastolic aortic pressure. The results of the comparison can be seen below in Figure 17 and Figure 18. For both sensitivity analysis, the computed sensitivity indices agree with one another, validating the implementation of the SGI method in MATLAB (MathWorks Version 2021a)

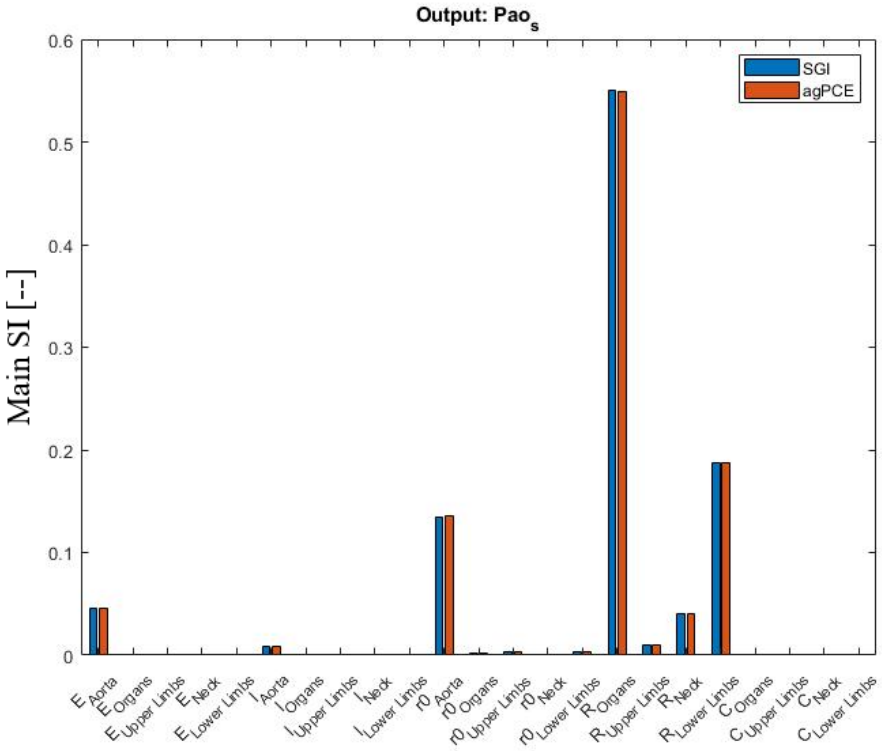

Figure 17: The comparison of computed variance contributions by the sensitivity analysis performed on the aortic systolic pressure as output by both the SGI and agPCE method.

[23] Koeppl et al., 2018, DOI:10.1002/cnm.3095
[24] Haasdonk and Santin, 2018, https://doi.org/10.1007/978-3-319-75319-5_2

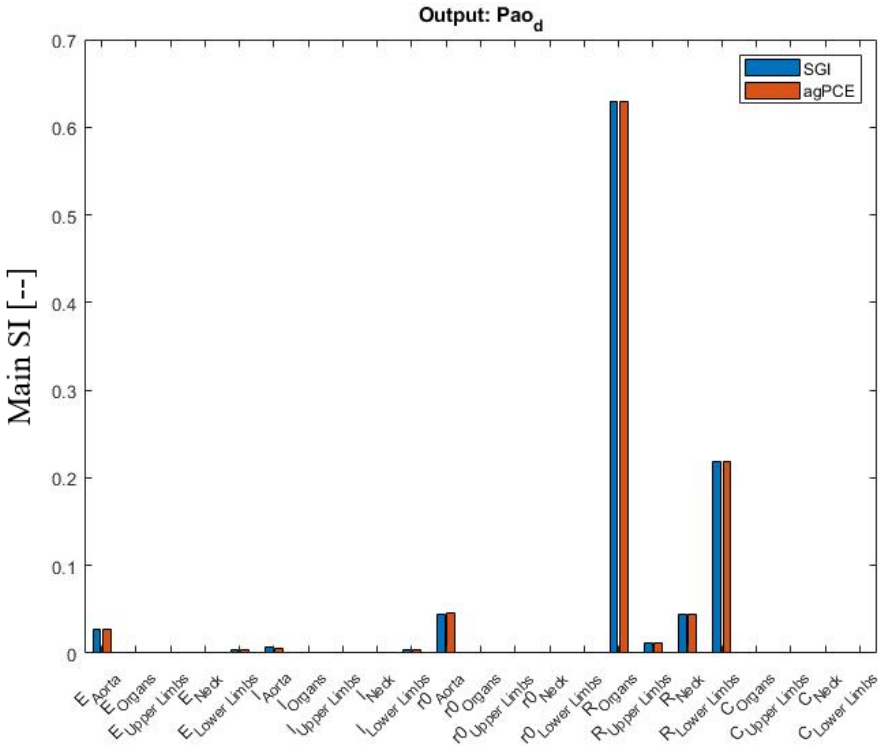

Figure 18: The comparison of computed variance contributions by the sensitivity analysis performed on the aortic diastolic pressure as output by both the SGI and agPCE method.

After the SGI method was validated, simulations were performed with correlations. Various simulations were run with increasing correlations between the following two input parameters: the length of the aorta and the radius of the aorta. The results of the variance contributions of certain input parameters on the computed pulse wave velocity of these simulations can be seen in Figure 19.

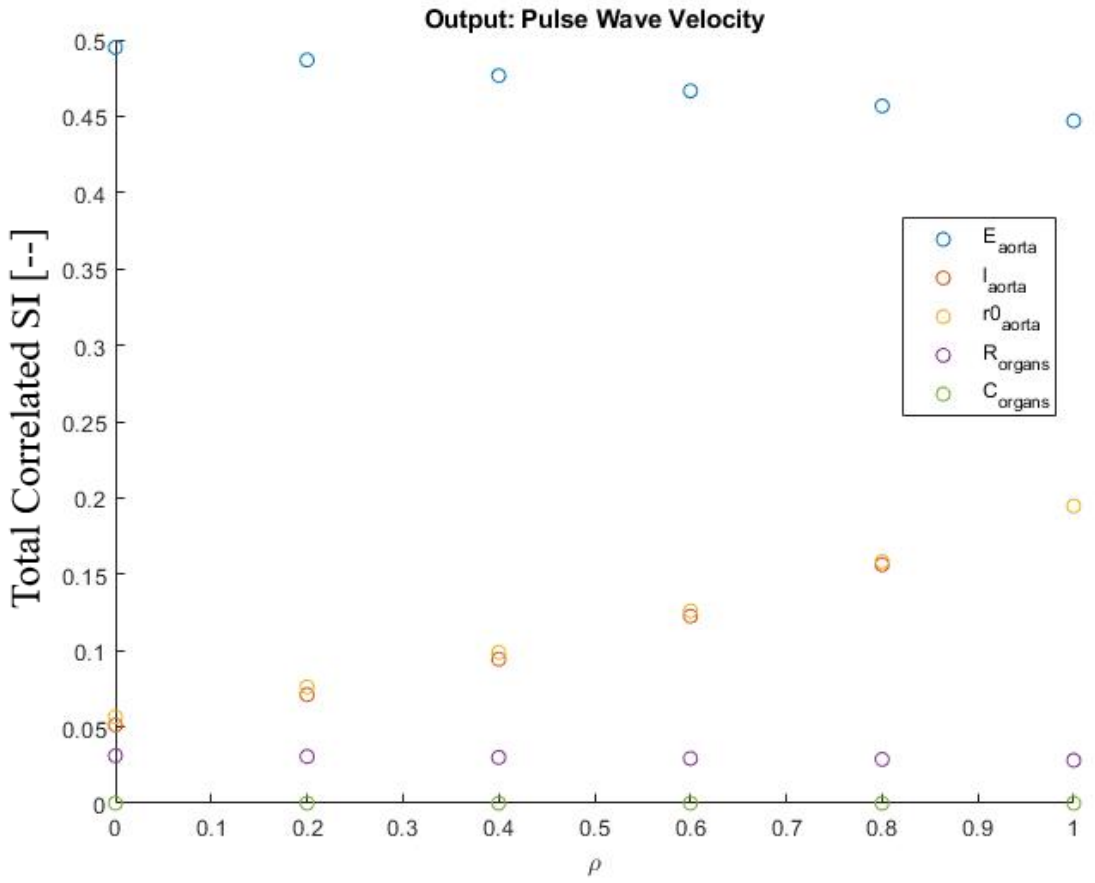

Figure 19: The comparison of computed variance contributions when the correlation between the aortic length and radius is increased.

As can be seen in Figure 19, increasing the correlations does affect the computed variance contributions of the aortic length and radius. Furthermore, it also affects the variance contribution of the uncorrelated aortic Young's Modulus. The peripheral resistance and compliance of the organs are unaffected by these changes in correlations between the aortic radius and length.

Discussion

In this section we have elaborated on an implementation to calculate sensitivity indices when inputs are statistically dependent. We have demonstrated that the methods have been implemented accurately, and that we are able to produce similar results as Li et al. In addition, we have applied our method to a cardiovascular 1D pulse wave propagation model, and we have shown the feasibility of the method also for this type of models. The emulator approach for fast evaluation of the 1D model gives similar results as when applying the method to the pulse wave propagation model directly. This approach is therefore also likely to be applicable to computational demanding models for which a proper surrogate model is derived.

Application of sensitivity toolbox

The sensitivity and uncertainty analysis tools presented in this deliverable will be further advanced and applied to the models of our use cases. First, we will now apply these techniques to our models (see *Deliverable 7.2 - First version of the simulation models (TUE, M9)*) to personalize and validate our models on patient-level, i.e.: Is the physiological model able to mimic the patient's physiology before and (later in the project) also after medical device implantation. The sensitivity analysis will in this stage mainly guide our measurement protocol and defines the relevant input space (the input space definition of *Deliverable 7.1 – Definition of model output (TUE, M6)* will be improved). The UQ tools will be use here to quantify the uncertainty due to uncertainties in the input.

Second, when patient-level validation has been done, virtual cohorts will be generated by varying model inputs simultaneously and subsequently evaluating our models (or their surrogates). Based on the outputs, and the filters that are designed on the RSA techniques presented in this deliverable, realistic virtual cohorts will be generated. The region of the output space that is considered as the behavioural set will be based on the output spaces of *Deliverable 7.3 – First version of the definition of the input space (TUE, M12)*.